

# Effect of condensation and evaporation on the viscous-convective subrange

Christopher A. Jeffery<sup>a)</sup>

*Atmospheric Sciences Programme, University of British Columbia, c/o #217 Geography, 1984 West Mall, U.B.C., Vancouver, BC, V6T 1Z2 Canada*

(Received 2 March 2000; accepted 1 December 2000)

The effect of condensation and evaporation on the viscous-convective subrange is investigated using a general mean-field approximation that is consistent with the nonhomogeneous vertical structure of the condensate's first and second moments and experimental observations of mean vertical flux in a condensation cloud. Expressions for the scalar density in the Batchelor limit are derived and used to reproduce the spectral behavior of new atmospheric measurements that exhibit anomalous scaling of cloud liquid water in the near inertial-convective regime. Good agreement between the model and data are obtained when axisymmetric Kraichnan transfer of scalar variance is balanced by axisymmetric production by condensation/evaporation resulting in an isotropic contribution to the real (homogeneous) part of the spectrum. The model also assumes a significant imaginary (nonhomogeneous) component to the spectrum that is indicative of a strong vertical coherence in condensation clouds. A "production subrange" is predicted in which the scalar dissipation rate increases with increasing wave number and the usual  $-1$  viscous-convective scaling evolves into an anomalous  $-3$  regime. The strongly nonhomogeneous (anisotropic) character of the predicted scalar spectrum is in stark contrast with atmospheric models of inertial-convective regime cloud inhomogeneity that are used in radiative transfer calculations and are typically isotropic. © 2001 American Institute of Physics. [DOI: 10.1063/1.1343481]

## I. INTRODUCTION

Recently, Davis *et al.*<sup>1</sup> presented horizontal spectra  $\phi(k_x)$  of cloud liquid water content (LWC) measured at an unprecedented resolution of 4 cm during the winter Southern Ocean Cloud Experiment (SOCEX). The scalar spectrum from the ensemble-average of the flight segments shown in Fig. 1 ( $\square$ ) exhibits two distinct scaling regimes: Kolmogorov scaling ( $-\frac{5}{3}$ ) is evident at larger scales and viscous-convective like scaling ( $-1$ ) is visible at the smallest scales. Although these spectral scalings are of no surprise, the scale break between the inertial-convective and viscous-convective regimes, estimated by Davis *et al.*<sup>1</sup> to occur at 2–5 m ( $k_b \approx 0.002 \eta^{-1}$ ,  $\eta =$  Kolmogorov length), is anomalous. Normal viscous-convective scaling, also shown in the figure ( $-$ ), intersects the inertial-convective subrange at  $k_b \approx 0.05 \eta^{-1}$  which corresponds to an  $r$ -space transition of around 10 cm in the atmosphere. Thus the observed scale break occurs at scales one order of magnitude larger than the standard theory predicts. What is particularly intriguing about these new observations are the implications for the scalar dissipation rate  $\chi$ ; with the new scale break,  $\chi$  in the viscous-convective regime is a factor of 14 larger than the inertial-convective  $\chi$ , suggesting that a source of scalar variance is present on scales of tens of centimeters.

Marshak *et al.*<sup>2</sup> suggests that the strong variability shown in Fig. 1 on scales of 4 cm to 4 m is consistent with Shaw *et al.*'s<sup>3</sup> discussion of a strong preferential concentration—the accumulation of inertial cloud droplets in

regions of high strain and low vorticity in a turbulent flow. However, a recent analysis of the effect of particle inertia on the viscous-convective subrange by the author<sup>4</sup> demonstrates that increased clumping of particles is associated with the suppression of viscous-convective scaling at near inertial-convective scales, i.e., the movement of  $k_b$  to smaller scales. Thus the data of Fig. 1 and the predictions in Ref. 4 are clearly at odds. Gerber *et al.*<sup>5</sup> suggests that the enhanced LWC variance at small scales is related to the small-scale entrainment features generated at cloud boundaries. However, as they admit, the spectral density distribution of entrainment scales and the in-cloud volume affected by entrainment and mixing are not known. Mazin<sup>6</sup> proposes that the non-inertial-convective scaling is caused by the temporal relaxation of the supersaturation to its steady-state value with e-folding time,  $\tau_p$ . Mazin argues that for updrafts with decorrelation time  $t \ll \tau_p$  the time is too short for a significant amount of phase change to occur and the turbulent laws for an inert scalar apply, whereas for  $t \gg \tau_p$  the supersaturation is close to its steady value and the cloud LWC behaves like an inert scalar with a vertical mean gradient. For time scales close to  $\tau_p$  the  $-\frac{5}{3}$  law is violated. However, two aspects of Mazin's hypothesis are questionable. First, the linear increase of LWC variability with height above cloud base demonstrates that a condensation cloud is fundamentally distinct from an inert scalar with an imposed mean gradient as discussed later, and that this distinction is present over a wide range of scales. Thus, the scaling for times  $t \gg \tau_p$  is just as likely to be anomalous as for times  $t \sim \mathcal{O}(\tau_p)$ . Second, it is not at all clear whether a change in the Lagrangian spectrum of supersaturation at temporal scales of  $\mathcal{O}(\tau_p)$  will, in fact,

<sup>a)</sup>Electronic mail: cjeffery@eos.ubc.ca

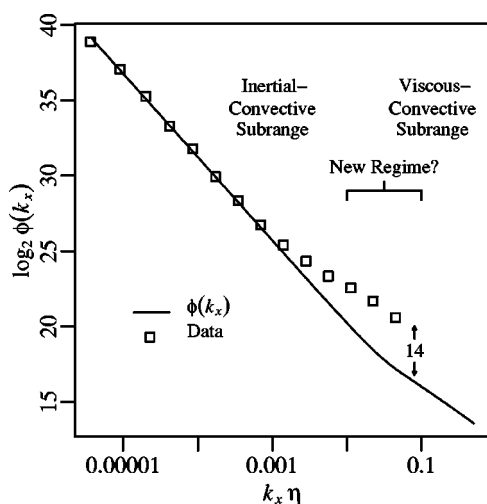


FIG. 1. Ensemble-averaged 1D scalar spectrum for cloud LWC data measured during the SOCEX field program and first presented in Ref. 2. A typical atmospheric value of 0.76 mm is assumed for the Kolmogorov length  $\eta$ . Also shown is the usual 1D inertial-convective/viscous-convective scaling calculated using  $q=5.5$  (Sec. IV) and  $\beta=3/4$  (Sec. VI). The observed spectrum is a factor of 14 greater than the normal spectrum in the viscous-convective regime.

lead to changes in the Eulerian spatial spectrum.

In this work, I propose that the anomalous scale break is caused by the effect of condensation and evaporation on scalar variance. Unlike other theories of condensation/evaporation effects on cloud microphysics, e.g., phase relaxation time<sup>6</sup> or buoyancy reversal,<sup>7</sup> the model proposed here does not invoke nonstationary, nonequilibrium, discrete or nonlocal phenomena such as sedimentation, buoyancy, entrainment or a noncontinuous droplet field. Rather, the present model is fundamentally a mean-field approximation that relates the complex process of condensation/evaporation to the mean vertical structure of liquid water in the cloud. Thus the present model is akin to Lagrangian parcel models where condensation/evaporation is largely dictated by the vertical velocity and the average environmental conditions inside the parcel. The present model decouples LWC production from the vapor and temperature fields, therefore, water vapor and temperature are represented by only their first moments through the equilibrium vertical liquid water structure. In fact, it should come as no surprise that anomalous viscous-convective scaling is observed in clouds if one considers that condensation/evaporation is an asymmetric internal pumping coupled to a large Reynolds number (Re), inertial velocity field that exhibits a continuous range of scales. As a result of this coupling, production of LWC will occur over a wide range of scales.

Conceptually, it is not hard to see how condensation through lifting can create liquid water variance. Consider a fluctuating (mean zero) variance  $\Theta(x)\Theta(y)$  where the vertical velocities  $u_3(x)$  and  $u_3(y)$  are both positive. As the parcel rises  $\Theta$  at both  $x$  and  $y$  increases through condensation, and the variance grows. Thus condensation/evaporation coupled to vertical advection leads to a self-excitation of LWC variance; in Sec. III we derive an advection-type

source term for the advection-diffusion equation of the form: source = velocity  $\times \partial(\Theta(x)\Theta(y))/\partial x_3$ .

The above example illustrates an important distinction between homogeneous, isotropic, incompressible mixing of a passive scalar in a reacting system (condensation cloud) and in an inert system with an initially imposed scalar gradient. The density fluctuations in the latter are stationary, anisotropic and homogeneous—properties that follow immediately from the incompressible advection-diffusion equation. Furthermore, the initial mean scalar gradient is maintained. In contrast, the density fluctuations in the former are stationary and anisotropic, but not homogeneous—mean-square density fluctuations increase in the direction of increasing mean density. Thus, although the mean density profiles of the two systems may be identical the statistical properties of the density fluctuations are not.

The present model, although limited to wavenumbers  $k \geq k_b$ , predicts that the LWC correlation function has an important nonhomogeneous, vertical contribution from a term linear in  $r_3$ . This general behavior agrees well with aircraft measurements<sup>8–10</sup> and numerical simulations<sup>11–13</sup> which demonstrate that both the mean and root-mean-square LWCs in atmospheric clouds increase linearly with height.

The closure used in this study to evaluate LWC covariance is appropriate for the viscous-convective subrange and was used in Ref. 4 to study the effect of particle inertia on spatial covariance. However, the results of this work are not directly applicable to the inertial-convective regime. Marshak *et al.*<sup>2</sup> have analyzed the radiative implications of an extended viscous-convective regime and found that LWC variability at scales less than the photon mean-free path (20–30 m) introduces an insignificant bias from complete homogeneity. This is not surprising considering that liquid water obeys inertial-convective scaling, and therefore most of the variability is contained in the largest scales. On the other hand, the results of this study, although limited to small scales, call into question the important and commonly made assumption of isotropy in the spatial statistics at large scales. In particular, the important vertical, nonhomogeneous component to the LWC correlation function predicted by the present model is, of course, anisotropic. The extent to which density fluctuations at larger scales may be considered locally isotropic may have important implications for radiative transfer.

Most radiative transfer calculations to date that incorporate LWC inhomogeneities assume isotropic variability. For example, Barker *et al.*<sup>14</sup> has developed a modeling technique where the inhomogeneity of the cloud field is calculated from a 1D time series of the extinction coefficient from aircraft measurements and then extended to three dimensions on the assumption of isotropic variability. His results suggest that internal homogeneity reduces cloud albedo and absorption. The above mentioned study by Marshak *et al.*<sup>2</sup> analyzes the radiative effects of sub-mean-free path liquid water variability using singular and bounded fractal models of LWC that are also isotropic. The importance of including internal variability in radiative transfer calculations is emphasized in Ref. 15.

Barker<sup>14</sup> justifies his assumption of isotropic variability

by commenting that ‘‘Since the corresponding temperature and liquid water content wave-number spectra follow  $k^{-5/3}$  closely, it may be safe to assume that the associated turbulence is approximately isotropic.’’ This statement implies a strong correspondence between local isotropy in the velocities and in the scalar field. However, it has recently been established<sup>16–22</sup> that the local isotropy central to Kolmogorov theory does not hold for a passive scalar field with an imposed mean gradient. In fact, a large anisotropy persists, even at very small scales and very high Reynolds numbers, and is evident in the skewness of the scalar derivative in the direction of the mean gradient. Pumir<sup>17</sup> compares the 1D spectra in the direction parallel and perpendicular to the mean gradient and finds clear differences. Although both spectra exhibit a limited inertial-convective subrange, differences persist from the smallest to the largest scales.

The present study suggests that in condensation clouds the dominant anisotropy in the spatial correlations is a manifestation of the nonhomogeneous vertical density fluctuations. To the best of my knowledge, the only radiative transfer calculations that incorporate vertically nonhomogeneous inhomogeneities are those of Hignett and Taylor<sup>23</sup> that are based on Barker’s<sup>14</sup> isotropic technique. Hignett and Taylor<sup>23</sup> model nonhomogeneous vertical LWC fluctuations by scaling the magnitude of the extinction coefficient with height above cloud base, and then compare the model predictions of reflectance and albedo with *in situ* aircraft radiometric observations of the same cloud. As in Ref. 14 they find that internal inhomogeneities lead to a reduction in cloud absorption and an increase in cloud transmittance.

The article is organized as follows. The source term representing condensation/evaporation is introduced in Sec. II, and in Sec. III the resulting equation for the correlation function in the Batchelor limit is derived. Also in Sec. III I present an approximate analytic form for the correlation function that illustrates the general anisotropic and nonhomogeneous properties of the full solution whose derivation follows in two parts. In Sec. IV, I derive a general axisymmetric solution for the spectral density without the new source term for both the viscous and inertial-convective subranges while the contribution from the new source term is determined in Sec. V. In Sec. VI the magnitude of the axisymmetric contributions to the spectral density are determined using the new data shown in Fig. 1. Sec. VII is a discussion of the predicted spectra, and Sec. VIII is reserved for conclusions.

## II. CONDENSATION/EVAPORATION SOURCE TERM

The density of a condensate  $\psi_c(t, \mathbf{x}) \in \mathbb{R}_+ = [0, \infty)$  in an incompressible velocity field is described by the advection-diffusion equation,

$$\frac{\partial \psi_c}{\partial t} + \mathbf{U} \cdot \nabla \psi_c = D_c \Delta \psi_c + \text{CE}(\psi_c \leftrightarrow \psi_v), \quad (1)$$

where  $\mathbf{U} = \mathbf{V} + \mathbf{u}$  is a random velocity field,  $\mathbf{V} = \langle \mathbf{U} \rangle$  is the mean velocity,  $D_c \in \mathbb{R}_+$  is the molecular diffusion coefficient and CE is a source term that models condensation ( $\psi_v \rightarrow \psi_c$ ) and evaporation ( $\psi_c \rightarrow \psi_v$ ) between the condensate

( $\psi_c$ ) and its vapor ( $\psi_v$ ). Condensation/evaporation occurs as a result of imposed vertical gradients ( $\hat{z} \equiv \hat{x}_3 \equiv \mathbf{e}_3$ ) in the temperature, pressure and vapor fields. Without loss of generality we can consider the case  $V_1 = V_2 = 0$  because of the Galilean invariance of Eq. (1). We will assume  $V_3 = 0$ . In general, CE is a function of  $\psi_c(t, \mathbf{x})$ ,  $\psi_v(t, \mathbf{x})$  and the macroscopic temperature field  $T(t, \mathbf{x})$  as well as a host of microscopic parameters including the saturation vapor-pressure, the diffusivity of heat and vapor and the latent heat of evaporation.<sup>24</sup> Furthermore, in a closed system CE is nonstationary because it is coupled through  $T(t, \mathbf{x})$  to irreversible thermodynamic processes, while, on the other hand, in an open system the spatial structure of CE has a non-trivial dependence on the thermal boundary conditions. To remove some of this complexity, we consider a simplified model for CE that is decoupled from both  $\psi_v$  and  $T$  and hence stationary, i.e., thermodynamics are reversible. The model is based on the following deterministic equation for the vertical structure of  $\psi_c$ :

$$\frac{\partial \psi_c}{\partial z} = \frac{p \psi_c}{z}, \quad (2)$$

where  $z(x_1, x_2)$  is the height above cloud base and  $p \in \mathbb{R}$  is a constant. Equation (2) states that  $\psi_c(\mathbf{x} + \Delta z)$  is related to its neighboring density  $\psi_c(\mathbf{x})$  through condensation ( $p > 0$ ) or evaporation ( $p < 0$ ), processes controlled by the vertical dependence of  $T$  and  $\psi_v$  which are assumed nonstochastic, i.e.,  $T(\mathbf{x}) = \langle T(z) \rangle$ . Thus Eq. (2) is a mean-field approximation, and as such, ignores nonlocal effects including entrainment of ‘‘non-cloud’’ environmental air at the boundaries of the system. The resulting vertical structure from (2),  $\langle \psi_c(z) \rangle \sim z^p$ , can be compared to experimental measurements of the system in question to determine the sign and magnitude of  $p$ . Using  $\partial/\partial z = \partial/\partial x_3 = u_3^{-1} \partial/\partial t$  gives

$$\text{CE} = \frac{p u_3}{z} \psi_c. \quad (3)$$

Note that the dependence  $\partial \psi_c / \partial t \sim u_3 \psi_c / z$  of (3) is also exhibited by Lagrangian parcel models of diffusional growth of water drops in clouds where  $\partial \psi_c / \partial t \sim (\psi_c / a) da / dt \sim \psi_c / t \sim w \psi_c / z$ ,  $a$  is the radius of the drop, and  $w$  is the vertical velocity of the parcel.<sup>24</sup> There are a number of experimental and numerical studies that report the vertical distribution of LWC inside stratus and stratocumulus clouds.<sup>8–13,25–27</sup> All these observations and model predictions show that the mean cloud liquid water increases nearly linearly with height from cloud base corresponding to  $p = 1$  in Eq. (2), and, therefore, the advection-diffusion equation for this system is

$$\frac{\partial \psi_c}{\partial t} + \mathbf{u} \cdot \nabla \psi_c = D_c \Delta \psi_c + \frac{u_3}{z} \psi_c. \quad (4)$$

In this work we examine the second-order ensemble mean moments of  $\psi_c$  as described by Eq. (4).

The ensemble-averaged advection-diffusion equation (1) with CE given by (3) does not predict  $\langle \psi_c(z) \rangle$ ; the connection between CE and the mean vertical structure of  $\psi_c$  follows from deterministic Eq. (2). However, using Eqs. (1) and (3) and assuming stationarity and horizontal homogeneity,

we find that the vertical flux of condensate obeys  $\langle u_3 \psi_c \rangle \sim z^p$ . Thus with an appropriate choice of  $p$ , the mean-field source term for condensation and evaporation (3) reproduces the experimentally observed vertical flux of condensate in the system of interest. Observational<sup>13,25,27</sup> and numerical studies<sup>13,28,29</sup> of atmospheric clouds demonstrate that the mean vertical flux of LWC is approximately linear in  $z$ , i.e.,  $p=1$  as above. The vertical dependence of  $\langle u_3 \psi_c \rangle$  is consistent with the discussion in Sec. I in that density fluctuations in a condensation cloud are nonhomogeneous.

### III. $\delta$ -CORRELATED CLOSURE

Motivated by the new experimental data discussed in Sec. I, we consider the small-scale, large Prandtl number (Pr) behavior of Eq. (4). It has been shown both numerically<sup>30,31</sup> and theoretically (see Ref. 4 and references therein) that the ‘‘correct’’ closure in this so called Batchelor limit is the  $\delta$ -correlated closure which predicts the well-known viscous-convective subrange.<sup>32</sup> The  $\delta$ -correlated model derives its name from the temporal properties of the velocity field which are assumed to rapidly decorrelate in time. A rapidly fluctuating velocity field can be derived formally through the velocity field renormalization  $\mathbf{u}_\epsilon(t, \mathbf{x}) = \epsilon^{-1} \mathbf{u}(\epsilon^{-2} t, \mathbf{x})$  where the molecular diffusivity  $D$  is not rescaled ( $D_\epsilon = D$ ) and where the long time rescaling  $\epsilon^{-2}$  is chosen to reproduce the conventional or normal diffusion  $\langle \mathbf{x}^2(t) \rangle \sim t$  associated with a mean field regime.<sup>33</sup> Under certain general conditions the random field  $\mathbf{u}_\epsilon(t, \mathbf{x})$  converges to a white noise process in the sense of distributions, i.e.,

$$\lim_{\epsilon \rightarrow 0} \langle \mathbf{u}_\epsilon(t+s, \mathbf{x}+\mathbf{r}) \mathbf{u}_\epsilon(t, \mathbf{x}) \rangle = 2\tau \delta(s) \langle \mathbf{u}_\epsilon(\mathbf{x}+\mathbf{r}) \mathbf{u}_\epsilon(\mathbf{x}) \rangle, \quad (5)$$

where  $\tau$  is the renewal time and  $r \ll l_0$  where  $l_0$  is the integral length scale. It follows trivially that the rescaled Eulerian correlation time  $\lim_{\epsilon \rightarrow 0} \tau_E \sim \epsilon^2$  is much less than molecular diffusion time, and, therefore, this renormalization corresponds to the large Pr limit.

The key simplification afforded by the  $\delta$ -correlated model is that the non-Markovian statistics of tracer trajectories arriving at  $(t, \mathbf{x})$  from neighboring points  $\mathbf{x} + \Delta \mathbf{x}$  and from past times  $t - \Delta t$  become Markovian, Eulerian statistics at  $(t, \mathbf{x})$ .<sup>4</sup> As a result, each of the tracer particles in an incompressible flow field undergoes an effective Brownian motion in this limit and the first- and second-order moments of the passive scalar field (ignoring any source terms) obey diffusion equations.<sup>34,35</sup> The diffusion equation for the second-order correlation function  $\Phi = \langle \Theta(\mathbf{x}) \Theta(\mathbf{y}) \rangle$  is<sup>4</sup>

$$\frac{\partial \Phi}{\partial t} = 2D_c \nabla^2 \Phi - 2[D_{mn}(0) - D_{mn}(\mathbf{r})] \frac{\partial^2 \Phi}{\partial x_m \partial y_n} + I, \quad (6)$$

where  $\Theta = \psi_c - \langle \psi_c \rangle$ ,  $I$  is the contribution from any source terms,  $\mathbf{r} = \mathbf{y} - \mathbf{x}$ , and  $D_{mn}(\mathbf{r}) = \langle \tau u_m(0) u_n(\mathbf{r}) \rangle$ . Note that the conventional Reynolds stresses  $\langle \Theta u_n \rangle \partial \langle \psi_c \rangle / \partial x_n$  that normally couple  $\Theta$  to mean-gradients in the passive scalar field do not contribute in the  $\delta$ -correlated model. Following the procedure outlined in Ref. 4 and references therein, the source term  $u_3 \psi_c / z$  of (4) in the rapid decorrelation in time limit becomes

$$I = 2[D_{3n}(0) - D_{3n}(\mathbf{r})] z^{-1} \frac{\partial \Phi}{\partial y_n}, \quad (7)$$

which has the form of an advection term. It is illustrative to compare the velocity  $V_{CE} = 2[D_{3n}(0) - D_{3n}(\mathbf{r})] z^{-1}$  with the velocity  $V_{PI} = 4 \partial D_{mn}(\mathbf{r}) / \partial r_n$  caused by particle inertia [Eq. (6) in Ref. 4]. Ignoring the anisotropic nature of the former, the two velocities scale according to  $V_{CE} \sim r^2$  and  $V_{PI} \sim r$  in the viscous regime, and  $V_{CE} \sim r^{2/3}$  and  $V_{PI} \sim r^{-1/3}$  in the inertial regime. Thus evaporation/condensation is a source of scalar variance that increases with increasing  $r$  (infrared divergence), whereas the effect of particle inertia is limited to scales  $\mathcal{O}(\eta)$ .

The general behavior of Eq. (6) with  $I$  given by (7) is worthy of some discussion. First, note that the viscous-convective scaling  $\Phi = \text{constant}$  is the trivial solution of (6) with or without the source term  $I$ . Thus a normal viscous-convective subrange is one prediction of the present model. However, a cloud with a vertical mean-gradient is axisymmetric about the  $e_3$  axis, and therefore we can expect  $\Phi$  to contain contributions from odd-order terms in  $r_3$ . Furthermore, the experimental data in Ref. 1 suggests that the nonhomogeneous vertical component of  $\Phi$  which does not contribute to the horizontal scalar spectrum disrupts normal viscous-convective scaling. Thus we can assume that there are other nontrivial contributions to  $\Phi$  in the viscous-convective regime. Second, note that since  $r \ll z$ ,  $z(x_1, x_2)$  can be treated as a constant parameter independent of  $r$ . If we assume that  $\Phi$  has a term  $\Phi' = c_1 z r_3$  with  $c_1 > 0$  which is consistent with aircraft measurements<sup>8-10</sup> and numerical simulations<sup>11-13</sup> that show increasing LWC fluctuations with increasing height, then  $I(\Phi')$  becomes

$$I(\Phi') = 2c_1 [D_{33}(0) - D_{33}(\mathbf{r})],$$

which is a positive source that increases with increasing  $r$ . The general form of the solution of Eq. (6) keeping terms greater than  $z^{-1}$  and ignoring molecular diffusion then becomes

$$\Phi(r, r_3, z) \approx c_0 + c_1 z r_3 + c_2 c_1 r_3^2 + c_3 c_1 r^2, \quad (8)$$

where  $c_0 > 0$  and the signs of  $c_2$  and  $c_3$  have yet to be determined. By definition the horizontal correlation function  $\Phi(r_1, r_2)$  as well as the horizontal viscous-convective spectral scaling is independent of  $r_3$ ; only the effects of the first and last terms in Eq. (8) are evident in horizontal measurements. It is important to emphasize that Eq. (8) is not the solution of Eq. (6) but only illustrates the general  $r$ - $z$  or in Fourier space  $\mathbf{k}$ - $z$  scaling that appears later when more rigorous methods are used. However, the picture that emerges from this analysis is robust—a nonhomogeneous component  $\sim r_3$  of  $\Phi$  that is  $z/r$  larger than the homogeneous components changes the normal  $k_{1,2}^{-1}$  horizontal viscous-convective spectral scaling.

### IV. AXISYMMETRIC KRAICHNAN TRANSFER

We begin the derivation of the spectral covariance density function  $\Psi(\mathbf{k}) = (2\pi)^{-3} \int d\mathbf{r} \Phi(\mathbf{r}) \exp(-i\mathbf{k} \cdot \mathbf{r})$  by considering the axisymmetric solutions of (6) without the source term  $I$ .

#### A. Viscous regime solution

Assuming the velocity field is divergenceless, homogeneous, and isotropic, the equal-time correlation function can be written<sup>4,36</sup>

$$\langle \tau u_m(\mathbf{x}) u_n(\mathbf{x} + \mathbf{r}) \rangle = D_T \left[ \delta_{mn} + \frac{r}{2} \frac{\partial F}{\partial r} \left( \delta_{mn} - \frac{r_m r_n}{r^2} \right) \right], \quad (9)$$

where  $D_T = u_0^2 \tau / 3$ ,  $u_0$  is the characteristic velocity of turbulent fluctuations with relaxation time  $\tau$ , and the function  $F(r)$  is the longitudinal correlation coefficient. In the viscous regime the following choice of parameters recovers the viscous-convective spectrum:<sup>4</sup>  $\tau = |\gamma|^{-1} / 6$ ,  $F(r) = 1 - \alpha(r/\eta)^2$ , and  $\alpha = \eta^2 / (12\tau^2 u_0^2)$  where  $\gamma = -(1/q)\tau_\eta^{-1}$  is the average value of the least principal rate of strain, and  $q$  is a universal constant for high Reynolds number flows.<sup>37</sup> Recent numerical simulations suggest  $q \approx 5.5$ .<sup>30,31</sup> Inserting Eq. (9) into (6) with viscous-regime correlation coefficients and  $I = 0$  gives

$$\frac{\partial \Phi}{\partial t} = 2D\nabla^2 \Phi + \frac{|\gamma|}{3} [2r^2 \delta_{mn} - r_m r_n] \frac{\partial^2 \Phi}{\partial r_m \partial r_n}, \quad (10)$$

which was first derived by Kraichnan.<sup>32</sup> The Fourier transform of (10) is easily found by using  $\partial/\partial r_j \rightarrow ik_j$ ,  $r_j \rightarrow i\partial/\partial k_j$  and then converting to axisymmetric variables where  $\theta = \cos^{-1}(\mathbf{k} \cdot \mathbf{e}_3 / |\mathbf{k}|)$  is the angle between the wave vector  $\mathbf{k}$  and the vertical axis:

$$\frac{\partial \Psi}{\partial t} = -2Dk^2 \Psi + \frac{|\gamma|}{3} T(\Psi), \quad (11)$$

$$T(\Psi) = k^2 \frac{\partial^2 \Psi}{\partial k^2} + 4k \frac{\partial \Psi}{\partial k} + \frac{2\cos\theta}{\sin\theta} \frac{\partial \Psi}{\partial \theta} + 2 \frac{\partial^2 \Psi}{\partial \theta^2}. \quad (12)$$

The isotropic solution of Eqs. (11) and (12) appeared first in Ref. 38 and is

$$\begin{aligned} \Psi^{\text{iso}}(k) &= \frac{\chi}{(2\pi)^{3/2} |\gamma|} \frac{\lambda^{3/2}}{k^{3/2}} K_{3/2}(\lambda k), \\ &= \frac{\chi}{4\pi |\gamma|} k^{-3} [1 + \lambda k] \exp(-\lambda k), \end{aligned} \quad (13)$$

$$\lambda = (6D|\gamma|^{-1})^{1/2}, \quad (14)$$

where  $K$  is a modified Bessel function,  $\chi(z) \sim z^2$  is the nonhomogeneous scalar dissipation rate and  $\lambda$  is a diffusive length scale that is proportional to the Batchelor length. For an isotropic scalar field the corresponding scalar spectrum  $E(k)$  is defined as  $E = 4\pi k^2 \Psi$ . Therefore in the range  $k \ll \lambda^{-1}$ ,  $E(k) = \chi |\gamma|^{-1} k^{-1}$  which is the usual  $k^{-1}$  viscous-convective scaling.

The general solution of Eqs. (11) and (12) can be obtained using the method of separation of variables:

$$\Psi(k, \mu) = \sum_{j=0}^{\infty} c_j B_j(k) P_j(\mu),$$

$$0 = (1 - \mu^2) \frac{\partial^2 P_j}{\partial \mu^2} - 2\mu \frac{\partial P_j}{\partial \mu} + j(j+1) P_j, \quad (15)$$

$$\lambda^2 k^2 B_j = k^2 \frac{\partial^2 B_j}{\partial k^2} + 4k \frac{\partial B_j}{\partial k} - 2j(j+1) B_j, \quad (16)$$

where  $\mu = \cos\theta$  and  $c_j \in \mathbb{C}$  is an arbitrary constant. Immediately we can identify  $P_j$  as a Legendre polynomial since Eq. (15) is the familiar Legendre equation.<sup>39</sup> The Fourier space symmetry relation  $\Psi(\mathbf{k}) = \Psi^*(-\mathbf{k})$  restricts the  $c_j$ 's such that for even  $j$ ,  $\text{Re}\{c_j\} \in \mathbb{R}_+$  and  $\text{Im}\{c_j\} = 0$ , whereas for odd  $j$ ,  $\text{Re}\{c_j\} = 0$ . Thus the odd terms represent the vertically nonhomogeneous component of the spectrum, whereas the even terms are homogeneous contributions. Note that for a passive scalar field in homogeneous turbulence with an imposed mean gradient the odd terms are identically zero.<sup>40</sup>

Equation (16) for  $B_j$  is a Bessel type equation with solution<sup>39</sup>  $B_j = k^{-3/2} K_{\nu(j)}(\lambda k)$  where  $\nu(j) = [9 + 8j(j+1)]^{1/2} / 2$ . Note that the  $P_j$ 's satisfy  $\int_{-1}^1 d\mu P_j(\mu) = 2\delta(j)$  so that only the  $j=0$  term contributes to the spherically averaged spectrum. The expansion of the scalar spectrum in terms of Legendre polynomials was first suggested by Herring<sup>41</sup> who derived an equation for  $\Psi$  in axisymmetric turbulence using Kraichnan's direct interaction approximation (DIA). The  $\delta$ -correlated model can be formally recovered from DIA in the limit that the Greens' function  $G(\mathbf{x}, t | \mathbf{y}, t | t_0)$ —the scalar amplitude at  $(\mathbf{x}, t)$  arising from a  $\delta$ -function source at  $t_0$  located in the fluid element that arrives at  $(\mathbf{y}, t)$ —becomes  $\delta^3(\mathbf{x} - \mathbf{y})$ .<sup>32</sup> Thus Eqs. (15) and (16) can be considered as a special case of the more general results in Ref. 41.

As discussed in Sec. III we are interested in the solution of the correlation function up to approximately second order in  $r_3$  which corresponds to expanding  $\Psi$  to  $j=2$ . The axisymmetric ( $j=1,2$ ) contribution to the spectral density,  $\Psi^{\text{axi}}$ , can be written

$$\Psi^{\text{axi}}(k, \mu) = \Psi_R^{\text{axi}}(k, \mu) + i\Psi_I^{\text{axi}}(k, \mu), \quad (17)$$

$$\Psi_R^{\text{axi}}(k, \mu) = \frac{c_2 \chi}{4\pi |\gamma|} \frac{2^{1-\nu} \lambda^{3/2}}{\Gamma(\nu)} K_\nu(\lambda k) P_2(\mu),$$

$$\Psi_I^{\text{axi}}(k, \mu) = \frac{\zeta \chi |\gamma|^{-1} z \lambda^{1/2}}{3(2\pi)^{3/2} k^{3/2}} K_{5/2}(\lambda k) P_1(\mu), \quad (18)$$

such that  $\lim_{k \rightarrow 0} \Psi_R^{\text{axi}}(k, \mu) = C \chi / (4\pi \gamma) \lambda^{3/2 - \nu} k^{-3/2 - \nu} \times P_2(\mu)$  and  $\lim_{k \rightarrow 0} \Psi_I^{\text{axi}}(k, \mu) = \zeta \chi / (4\pi |\gamma|) z \lambda^{-2} k^{-4} \times P_1(\mu)$ , and where  $\nu = \sqrt{57}/2 \approx 3.775$ . The constant  $\zeta$  in Eq. (18) is of fundamental importance in what follows and plays the role of the Kolmogorov constant for the nonhomogeneous (imaginary) component of the spectral density. As discussed in Sec. III the nonhomogeneous component  $\Psi_I^{\text{axi}}$  is assumed to scale as  $zk$  times the homogeneous components

$\Psi^{\text{iso}}$  or  $\Psi_R^{\text{axi}}$  as illustrated in Eq. (18). The resulting  $r$ -space scalings are given by Eq. (17):  $r$  and  $r^{2.275}$  are close to the  $r$  and  $r^2$  scaling estimated in Sec. III.

### B. Inertial-convective regime solution

A solution for  $\Psi$  in the inertial-convective subrange  $r > \eta$  is facilitated by the fact that the molecular diffusivity can be ignored in this regime. Evaluating Eq. (6) with (9) and velocity correlation coefficient  $F(r) = 1 - \alpha_2 r^{2/3}$  where  $\alpha_2$  is an arbitrary constant gives

$$[4r^2 \delta_{mn} - r_m r_n] \frac{\partial^2 \Phi}{\partial r_m \partial r_n} = 0,$$

which can be Fourier transformed as before:

$$12\Psi + 3k^2 \frac{\partial^2 \Psi}{\partial k^2} + 16k \frac{\partial \Psi}{\partial k} + \frac{4 \cos \theta}{\sin \theta} \frac{\partial \Psi}{\partial \theta} + 4 \frac{\partial^2 \Psi}{\partial \theta^2} = 0.$$

Expanding the solution in terms of Legendre polynomials gives

$$\Psi(k, \mu) = \sum_{j=0}^{\infty} B_j(k) P_j(\mu),$$

$$0 = 3k^2 \frac{\partial^2 B_j}{\partial k^2} + 16k \frac{\partial B_j}{\partial k} - [4j(j+1) - 12] B_j,$$

with solution  $B_j = k^{-13/6} [c_j k^{-\nu(j)} + d_j k^{\nu(j)}]$  where  $\nu(j) = \{169 + 12[4j(j+1) - 12]\}^{1/2}/6$ , and  $c_j$  and  $d_j$  are arbitrary constants. In general both  $c_j$  and  $d_j$  are nonzero; however, in the small  $k$  viscous-convective regime  $k^{-\nu(j)} \gg k^{\nu(j)}$ , and therefore without loss of generality we can set  $d_j = 0$ . Note that the scaling of the isotropic ( $j=0$ ) solution  $\Psi^{\text{iso}} \sim k^{-3}$  is invariant under a change in the velocity spatial correlation, a manifestation of the fact that  $\Phi = \text{constant}$  is the trivial solution of Eq. (6) independent of the effective diffusivity. In addition, the scaling of the ( $j=1$ ) solution  $\Psi_I^{\text{axi}} \sim k^{-4}$  also remains invariant. The scaling of  $\Psi_R^{\text{axi}}$  ( $j=2$ ) changes only slightly from a viscous scaling of  $\approx -5.275$  to an inertial scaling of  $-(13 + \sqrt{313})/6 \approx -5.115$ . Because of the steeper spectral decay of the axisymmetric contribution,  $\Psi^{\text{iso}} \gg \Psi_R^{\text{axi}}$  for  $k > \eta^{-1}$ , and therefore, only the  $k^{-5.115}$  scaling makes a significant contribution to the overall spectral density. Using the approximation  $k^{-5.115} \approx k^{-5}$ ,  $\Psi_R^{\text{axi}}$  can be written

$$\Psi_R^{\text{axi}}(k, \mu) = \frac{c_2 \chi}{4\pi |\gamma|} \lambda^{-2} k^{-5} P_2(\mu), \quad (19)$$

which corresponds exactly with the  $r$ -space scaling of the last two terms in Eq. (8). Equations (18) and (19) are used in the rest of this work to represent axisymmetric viscous-convective scaling.

### V. THE AXISYMMETRIC SOURCE I

The contribution of the axisymmetric, real term  $\Psi_R^{\text{axi}}$  to the overall spectral density in the absence of the condensation/evaporation source  $I$  is fundamentally limited by the restriction  $\text{Re}\{\Psi\} \geq 0$ . Using  $P_2(\mu) = (3\mu^2 - 1)/2$  and an inertial-convective/viscous-convective boundary at  $k$

$= k_b$  this restriction becomes  $\Psi^{\text{iso}}(k_b) \geq \Psi_R^{\text{axi}}(k_b, \mu = 0, \pm 1)$ . For example, using the spectra  $\Psi^{\text{iso}} = k^{-3}$ , the maximum allowed anisotropy  $\Psi_R^{\text{axi}} = B_2(k) P_2(\mu)$  where  $B_2(k) = 2k^{-5} k_b^2$ , and the identities for the 1D horizontal spectra  $\phi^{\text{iso}}(k_x) = 4\pi \int_{k_x}^{\infty} k dk \Psi^{\text{iso}}(k)$  and  $\phi^{\text{axi}}(k_x) = \pi \int_{k_x}^{\infty} k dk (1 - 3k_x^2/k^2) B_2(k)$  gives  $\phi^{\text{iso}}(k_x) = 4\pi k_x^{-1}$  and  $\phi^{\text{axi}}(k_x) = -8\pi/15 k_x^{-3} k_b^2$ . Thus the maximum possible change in the horizontal spectrum which occurs at the boundary  $k = k_b$  is only  $\frac{2}{15}$  or about 13%! The physical interpretation of these results is straightforward. The solution  $\Psi_R^{\text{axi}}$  represents a conservative transfer or rotation of scalar variance along the  $e_3$  axis, and thus in the absence of a source, little rotation is possible before the variance becomes depleted at  $\mu = 0$  or  $\pm 1$ . The source term  $I$ , therefore, plays a crucial role in balancing this anisotropic conservative spectral transfer.

The equation for  $\Psi$  in the viscous regime (10) including the source term (7) is

$$\frac{\partial \Phi}{\partial t} = 2D \nabla^2 \Phi + \frac{|\gamma|}{3} [2r^2 \delta_{mn} - r_m r_n] \frac{\partial^2 \Phi}{\partial r_m \partial r_n} + \frac{|\gamma|}{3z} [2r^2 \delta_{3n} - r_3 r_n] \frac{\partial \Phi}{\partial r_n}.$$

Fourier transforming as per Eq. (11) produces

$$\frac{\partial \Psi}{\partial t} = -2Dk^2 \Psi + \frac{|\gamma|}{3} T(\Psi) - \frac{i|\gamma|}{3} P(\Psi),$$

$$P(\Psi) = \frac{\cos \theta}{z} \left\{ k \frac{\partial^2 \Psi}{\partial k^2} + 4 \frac{\partial \Psi}{\partial k} + \left[ \frac{2 \cos \theta}{k \sin \theta} - \frac{\sin \theta}{k \cos \theta} \right] \frac{\partial \Psi}{\partial \theta} + \frac{\sin \theta}{\cos \theta} \frac{\partial^2 \Psi}{\partial \theta \partial k} + \frac{2}{k} \frac{\partial^2 \Psi}{\partial \theta^2} \right\},$$

where  $T(\Psi)$  is given by (12). The equation for the spectral contribution  $\Psi^{\text{src}}$  from the source  $I$  is

$$\frac{\partial \Psi^{\text{src}}}{\partial t} = -2Dk^2 \Psi^{\text{src}} + \frac{|\gamma|}{3} T(\Psi^{\text{src}}) - \frac{i|\gamma|}{3} P(i\Psi_I^{\text{axi}}). \quad (20)$$

Using (18) the source term becomes

$$P(i\Psi_I^{\text{axi}}) = i[P_c(\Psi_I^{\text{axi}}) \cos^2 \theta + P_s(\Psi_I^{\text{axi}}) \sin^2 \theta],$$

$$P_c(\Psi_I^{\text{axi}}) = \frac{\zeta \chi}{3(2\pi)^{3/2} |\gamma|} \frac{\lambda^{5/2}}{k^{1/2}} K_{5/2}(\lambda k),$$

$$P_s(\Psi_I^{\text{axi}}) = \frac{\zeta \chi}{3(2\pi)^{3/2} |\gamma|} \frac{\lambda^{3/2}}{k^{3/2}} K_{7/2}(\lambda k).$$

Note that for small  $k$ ,  $P_c \ll P_s$  and  $P_s(\Psi_I^{\text{axi}}) = 5\zeta \chi / (4\pi |\gamma|) \lambda^{-2} k^{-5}$ . Therefore the small  $k$ , steady-state equation analogous to (20) is

$$T(\Psi^{\text{src}}) + \frac{5\zeta \chi}{4\pi |\gamma|} \lambda^{-2} k^{-5} \sin^2 \theta = 0. \quad (21)$$

Assuming a solution of the form  $\Psi^{\text{src}} = (A + B\mu^2)k^{-5}$  and evaluating (21) gives  $-2B = -10A - 4B = 5\zeta \chi / (4\pi |\gamma|) \times \lambda^{-2}$  or

$$\Psi^{\text{src}}(k, \mu) = -\frac{\zeta \chi}{4\pi|\gamma|} \lambda^{-2} k^{-5} \frac{1}{2} (5\mu^2 - 1).$$

Not surprisingly, this solution is invariant under the transformation from inertial to viscous velocity correlations (not shown). Assuming that the sum of the axisymmetric, real terms  $\Psi_R^{\text{axi}}$  (19) and  $\Psi^{\text{src}}$  is approximately isotropic gives  $c_2 = 5/3\zeta$ , and the resulting spectral density is

$$\Psi_R^{\text{axi}} + \Psi^{\text{src}} = -\frac{\chi}{4\pi|\gamma|} \frac{\zeta}{3} \lambda^{-2} k^{-5}. \quad (22)$$

Thus axisymmetric production of scalar variance ( $\Psi^{\text{src}}$ ) is balanced by a conservative axisymmetric transfer of scalar variance ( $\Psi_R^{\text{axi}}$ ) producing a resulting spectral density that is isotropic. An assumption of perfect isotropy is not necessary to prevent the spectral density from becoming negative. However, a small degree of anisotropy in  $\Psi_R^{\text{axi}} + \Psi^{\text{src}}$  has little effect on the results and conclusions in the following sections. Combining Eqs. (13) and (22) gives the resultant spectral density

$$\begin{aligned} \Psi(k, \mu) &= \Psi^{\text{iso}}(k) + [\Psi_R^{\text{axi}} + \Psi^{\text{src}}](k) + i\Psi_I^{\text{axi}}(k, \mu, \zeta), \\ &= \frac{\chi}{4\pi|\gamma|} k^{-3} [1 + \lambda k] \exp(-\lambda k) \\ &\quad - \frac{\chi}{4\pi|\gamma|} \frac{\zeta}{3} \lambda^{-2} k^{-5} + i\Psi_I^{\text{axi}}(k, \mu, \zeta), \end{aligned}$$

where  $\Psi_I^{\text{axi}}$  is given by (18). The spectrum  $E(k) = 2\pi k^2 \int_{-1}^1 d\mu \Psi(k, \mu)$  is therefore

$$E(k) = \frac{\chi}{|\gamma|} k^{-1} [1 + \lambda k] \exp(-\lambda k) - \frac{\chi}{|\gamma|} \frac{\zeta}{3} \lambda^{-2} k^{-3}. \quad (23)$$

Comparing Eq. (23) with (8) we find that  $c_2 = 0$  as a result of the isotropic assumption (above). The Kolmogorov-like constant  $\zeta$  first introduced in Sec. IV A is determined in the next section.

## VI. DETERMINATION OF $\zeta$

The only free parameter in the present model is the fundamental constant  $\zeta$  defined by Eq. (18). Like the Kolmogorov constant,  $\zeta$  should asymptote to a well-defined value in the large Re limit. Since independent information on  $\zeta$  is not yet available in the literature, its value is chosen to best reproduce the experimental data shown in Fig. 1.

The time-evolution equation for the spherically integrated scalar covariance spectrum  $E(k) = 2\pi k^2 \times \int_{-1}^1 d\mu \Psi(k, \mu)$  may be written as<sup>4</sup>

$$\frac{\partial E(k)}{\partial t} = -\frac{\partial \chi(k)}{\partial k} - 2Dk^2 E(k) + F(k),$$

where  $F(k)$  is the production spectrum of scalar variance. Solving for  $\chi$  in the steady state for the range  $k \ll \lambda^{-1}$  gives

$$\chi(k) \approx \chi_0 - \int_k^\infty F(\xi) d\xi, \quad (24)$$

where  $\chi_0 = 2D \int_0^\infty k^2 E(k) dk$ . Equation (24) was used by Mjolsness<sup>38</sup> with  $F = 0$  to derive the constant of proportion-

ality, i.e.,  $\chi/(4\pi|\gamma|)$  where  $\chi = \chi_0$ , in (13) which agrees well with numerical simulations.<sup>30,31</sup> Phillips<sup>42</sup> used (24) where  $F$  is the spectrum of the conventional Reynolds stress term  $\langle bw \rangle \partial \langle b \rangle / \partial z$  and  $b$  is the buoyancy  $-g\psi/\langle \psi \rangle$ , along with the earlier results of Lumley<sup>43</sup> to derive the buoyancy (temperature) spectrum in a stably stratified fluid. Phillips' derivation was corrected by Weinstock<sup>44</sup> who showed that the Lumley–Phillips buoyancy subrange theory predicts the temperature spectrum is proportional to  $k^{-3}$  at small  $k$ —consistent with experiments. Recently, I used (24) to derive the magnitude of  $E$  in the viscous-convective subrange where the production  $F$  is caused by particle inertia.<sup>4</sup>

The determination of  $F$  in this study is complicated by the fact that an expression is needed that is accurate in both the viscous  $k > \eta^{-1}$  and inertial  $k < \eta^{-1}$  regimes. The viscous regime form  $F_v$  follows from Eq. (21):

$$\begin{aligned} F_v(k) &= 2\pi k^2 \int_0^\pi \sin \theta d\theta \frac{5\zeta \chi}{12\pi} \lambda^{-2} k^{-5} \sin^2 \theta \\ &= \frac{10\zeta \chi}{9} \lambda^{-2} k^{-3}. \end{aligned}$$

The scale break between the viscous and inertial regimes  $k_i$  is usually taken to be around  $0.1\eta^{-1}$ . Thus for  $k < k_i$  we can expect the inertial scaling  $F_i(k) \sim k^{-5/3}$  where  $F_i(k_i) = F_v(k_i)$ . The resulting expression for  $\chi$  using Eq. (24) is

$$\chi(k) = \begin{cases} \chi_0 - \frac{5\zeta \chi_0}{3\lambda^2 k_i^{4/3}} [k^{-2/3} - (2/3)k_i^{-2/3}], & k \leq k_i, \\ \chi_0 - \frac{5\zeta \chi_0}{9\lambda^2 k^2}, & k > k_i. \end{cases} \quad (25)$$

The unknown constant  $\zeta$  can be determined from Eq. (25) in principle using the new liquid water data in Ref 1. One source of uncertainty, however, is the magnitude of the Obukhov–Corrsin constant  $\beta$  in the inertial-convective regime parametrization

$$E_{\text{ic}}(k) = \beta \chi_{\text{ic}} \varepsilon^{-1/3} k^{-5/3}, \quad (26)$$

where  $\varepsilon$  is the energy dissipation rate and  $\chi_{\text{ic}} = \text{constant}$  is the inertial-convective range scalar dissipation rate. Since the change in  $\beta$  due to condensation/evaporation is unknown, we assign  $\beta$  its inert passive scalar value of  $\approx \frac{3}{4}$ . Using the data in Ref. 1 I estimate that  $\chi_{\text{ic}} \equiv \chi(k_b) = \chi_0/14$  which gives

$$\zeta = \frac{39}{70} \lambda^2 k_i^{4/3} [k_b^{-2/3} - (\frac{2}{3})k_i^{-2/3}]^{-1}, \quad (27)$$

where  $k_b$  is the wave number of the scale break between the inertial-convective and viscous-convective regimes. Substituting Eq. (27) into (23) with the identification  $\chi \rightarrow \chi_0$  gives

$$\begin{aligned} E(k) &= \frac{\chi_0}{|\gamma|} k^{-1} [1 + \lambda k] \exp(-\lambda k) \\ &\quad - \frac{13}{70} \frac{\chi_0}{|\gamma|} k_i^{4/3} [k_b^{-2/3} - (2/3)k_i^{-2/3}]^{-1} k^{-3}. \end{aligned} \quad (28)$$

The final step in the specification of  $E$  is the determination of  $k_b$ . Numerical simulations<sup>30,31</sup> of the viscous-convective

subrange with  $F=0$  suggest that the scale break  $k_b$  occurs, naturally, at the intersection  $E_{ic}(k_b)=E(k_b)$  which can be calculated numerically from (26) and (28). Using  $\beta=\frac{3}{4}$ ,  $k_i=0.1\eta^{-1}$  and recalling from Sec. IV A that  $\gamma=-(1/q)\tau_\eta^{-1}$  where  $q=5.5$  produces  $k_b=0.04\eta^{-1}$ . Thus the predicted scale break between the inertial-convective and viscous-convective regimes is at somewhat larger scales than the usual break at  $k_b=(\beta/q)^{3/2}\eta^{-1}\approx 0.05\eta^{-1}$ . This extension to larger scales can be contrasted with the effect of particle inertia which suppresses near-inertial viscous-convective scaling.<sup>4</sup> In the atmosphere where  $\eta\sim\mathcal{O}(1\text{ mm})$ , the predicted  $\mathbf{r}$ -space scale break occurs around 25 cm which is an order of magnitude smaller than the transition estimated by Davis *et al.*<sup>1</sup> to occur at 2–5 m. This apparent discrepancy is discussed further in the next section. Equations (25)–(28) complete the determination of  $E(k)$  as a function of the parameters  $\chi_0$ ,  $|\gamma|$ ,  $\lambda$ ,  $k_i$  and  $k_b$ .

**VII. SPECTRA AND DISCUSSION**

Before embarking on a discussion of the predictions of the present model, it should be emphasized that these predictions are highly dependent on the value of the Kolmogorov-like parameter  $\zeta$  [Eq. (18)]. In particular, in the limit  $\zeta\rightarrow 0$  normal  $k^{-1}$  viscous convective scaling is recovered. Despite this deficiency, the present model provides an appealing analytical framework within which the anomalous scaling of cloud LWC can be explained.

In the region  $(k_b=0.04\eta^{-1})\leq k\leq 0.35\eta^{-1}$  the scalar dissipation rate increases with increasing  $k$  according to Eq. (25). A typical atmospheric value for  $\eta$  is  $\approx 1$  mm, and therefore, this ‘‘production subrange’’ corresponds to scales of about 3 cm up to 30 cm. At smaller scales ( $r<3$  cm) a normal viscous-convective subrange exists associated with a constant scalar dissipation rate  $\chi_0$  and at larger scales ( $r>30$  cm) the cascade of variance from larger to smaller scales dominates the dynamics. In the production subrange the spectral scaling changes from a negatively sloped  $k^{-1}$  scaling to a positively sloped  $k^{-3}$  scaling [Eq. (28)], reflecting the production of scalar variance in the vicinity of  $k_b$ .

The scalar spectrum given by Eqs. (25)–(28) is shown in Fig. 2 along with the change in scalar dissipation rate  $\chi(k)/\chi_{ic}$ . The increase in the variance beginning at  $k=k_b$  is associated with a corresponding increase in the scalar dissipation rate. Outside of the production subrange normal inertial-convective and viscous-convective behavior is evident. The bump in the scalar spectrum in the production subrange—a reflection of increased variance in this regime—is superficially similar to the spectral bump caused by particle inertia (Fig. 5 in Ref. 4). The location of the spectral peak at  $k_p\approx 0.033\eta^{-1}$  in the present model represents increased variance at scales one order of magnitude larger than preferential concentration ( $k_p\approx 0.3\eta^{-1}$ ), a relationship mirrored by the behavior of the condensation/evaporation induced velocity  $\langle\tau u(0)u(\mathbf{r})\rangle/z$  compared to the particle inertia induced velocity  $\langle\tau u(0)\nabla\cdot u(\mathbf{r})\rangle$ . Despite some similarities between Figs. 2 and 5 in Ref. 4, the physics of condensation/evaporation and preferential concentration is distinctly different. Preferential concentration is an accumu-

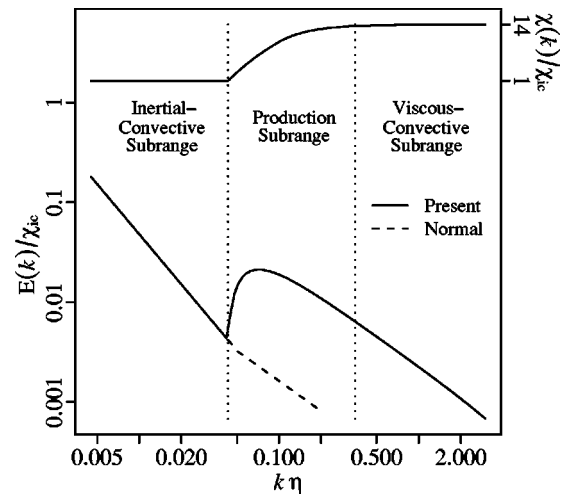


FIG. 2. Plot showing the inertial-convective, production and viscous-convective subranges predicted by the present model [Eqs. (25)–(28)]. The production subrange begins at  $k_b=0.04\eta^{-1}$  and is associated with increasing scalar production and dissipation. The increase in  $\chi$  by a factor of 14 presented at the top of the figure is chosen to reproduce the 1D LWC spectrum measured during SOCEX and shown in Fig. 3. Normal inertial-convective/viscous-convective scaling is also shown for comparison. The figure is generated using  $\varepsilon=0.01\text{ m}^2\text{ s}^{-3}$ .

lation or clumping of inertial particles in regions of high strain and low vorticity in a turbulent flow and, therefore, by definition, is a manifestation of a nonuniform particle distribution. In contrast, the increased variance exhibited by the present model assumes a uniform particle distribution but allows for variable particle mass due to condensation and evaporation.

The 1D horizontal spectrum defined by  $\phi(k_x)=\int_{k_x}^{\infty} k^{-1}dkE(k)$  is shown in Fig. 3 along with the experimental data from Ref. 1. The good agreement between the modeled and observed spectra for  $k\approx 0.04\eta^{-1}$  is not

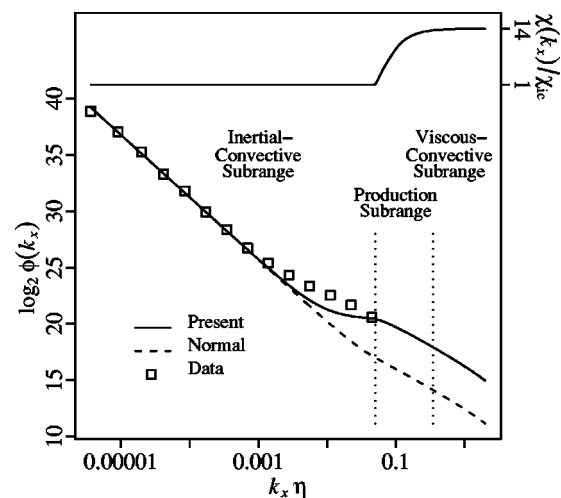


FIG. 3. Comparison of the ensemble-averaged 1D LWC scalar spectrum measured during SOCEX<sup>2,1</sup> and the present model [Eqs. (25)–(28)]. The factor of 14 increase in  $\chi(k=k_x)$  in the production subrange is chosen to produce good agreement between  $\phi(k_x)$  and the data at large  $k_x$ . The discrepancy in the modeled and observed spectra near  $k_x=0.008\eta^{-1}$  may be a result of the unnaturally sharp transition between the inertial-convective and production regimes shown in Fig. 2 and used in the generation of  $\phi(k_x)$ .

fortuitous—the relation  $\chi_{ic} = \chi_0/14$  used in Sec. VI to determine the unknown constant  $\zeta$  was chosen to produce a close correspondence between the two spectra in this region. For  $k$  in the range  $0.002\eta^{-1} < k < 0.04\eta^{-1}$  the modeled spectrum falls somewhat below the experimental data. The plateau in the modeled spectrum near  $k = k_b$  is associated with the sharply defined local minimum exhibited by  $E$  in the same region and shown in Fig. 2. It is very likely that the real transition between the inertial-convective and production regimes is much smoother than the prediction of the present model which may explain the discrepancy between the 1D spectra shown in Fig. 3. The plateau in the modeled spectrum near  $k = k_b$  may also explain the discrepancy between the 25 cm scale break ( $k_b = 0.04\eta^{-1}$ ) predicted by the present model and the break estimated by Davis *et al.*<sup>1</sup> from experimental data (Fig. 3) to occur at 2–5 m ( $k_b \approx 0.002\eta^{-1}$ ). Certainly, since  $\phi(k_x)$  is a projection of the actual 3D spectral density  $\Psi(k)$ , an abrupt change in the scaling of  $\Psi$  (or  $E$ ) appears smooth and gradual when projected onto  $k_x$ . Thus, the appearance of  $\phi(k_x)$  is not necessarily a reliable indicator of the behavior of  $E(k)$ . Overall, the experimental data in Ref. 1 does support the existence of a production subrange predicted by the present model (25)–(28).

The key assumption in the derivation of the production subrange is the existence of the imaginary spectral density  $\Psi_I^{\text{axi}}$  (18) that goes as  $zk^{-4}\mu$  for small  $k$ . Because  $\Psi_I^{\text{axi}}$  scales with an integer exponent the  $r$ -space contribution cannot be calculated without knowledge of a transition from the  $k^{-4}$  scaling to a different (noninteger) scaling regime. Clearly, more information on the spectral density of liquid water in clouds from numerical simulations is needed to ascertain the validity of the scaling and magnitude of  $\Psi_I^{\text{axi}}$  used in the present model.

## VIII. CONCLUSIONS

A mean-field model for the effect of condensation and evaporation on passive scalar statistics is developed that relates the phase change of the condensate to the vertical structure of its first and second moments in the cloud. Unlike inert scalar statistics with an initially imposed scalar gradient, the new model predicts nonhomogeneous vertical density fluctuations—in good agreement with atmospheric measurements<sup>8–10</sup> and numerical simulations<sup>11–13</sup> that show increasing liquid water fluctuations with increasing height in clouds. As a first step towards understanding the effect of condensation/evaporation on passive scalar statistics, an equation for the spectral density  $\Psi$  is derived in the viscous-convective regime where an exact closure is available. The derivation proceeds in two parts: the axisymmetric spectral contribution in the Batchelor limit, derived for both viscous and inertial velocity correlations, is written as an infinite sum of Legendre polynomials of  $\mu$  as first suggested by Herring;<sup>41</sup> the first-order contribution from condensation/evaporation is also derived assuming that the imaginary (nonhomogeneous) part of  $\Psi$  is significantly large. In the absence of condensation/evaporation axisymmetric Kraichnan transfer of scalar variance is virtually forbidden because

of the restriction that the real part of  $\Psi$  be positive. However, in the presence of condensation/evaporation the possibility of axisymmetric transfer balancing axisymmetric production of variance to produce an isotropic, homogeneous contribution  $E(k) \sim k^{-3}$  exists and is explored.

Under the assumption of spectral balance, an expression for  $\Psi$  is derived that reproduces the spectral behavior of new experimental data of cloud liquid water density<sup>1</sup> which exhibits anomalous viscous-convective scaling. The modeled spectrum has one adjustable constant reflecting the magnitude of the imaginary (nonhomogeneous) part of the spectrum; the value of this constant is chosen judiciously so that good agreement is obtained between the observed and modeled horizontal spectra. The present model predicts a production subrange,  $0.04\eta^{-1} \leq k \leq 0.35\eta^{-1}$ , where the scalar dissipation rate increases with increasing  $k$ . Associated with increased dissipation is a change in the spectral scaling from the usual negatively sloped  $k^{-1}$  viscous-convective scaling to an anomalous positively sloped  $k^{-3}$  regime. The resulting scalar spectrum in the production subrange has a well defined bump reflecting increased variance due to condensation and evaporation, similar to the behavior exhibited in the spectrum of inertial particles.<sup>4</sup> The scale break between the inertial-convective and production (viscous-convective) subrange occurs at  $0.04\eta^{-1}$ —slightly smaller than the usual transition near  $0.05\eta^{-1}$  for an inert scalar—although the break in the 1D horizontal spectrum remains consistent with data and Davis *et al.*'s<sup>1</sup> somewhat larger-scale estimate. Despite some uncertainty in the vicinity of the inertial-convective/production subrange transition, the present model provides a convenient analytic framework within which the nonhomogeneous, anisotropic behavior of condensation cloud spectral scaling may be explored.

The initial success of the mean-field model notwithstanding, a number of important questions remain unanswered. In particular, the predicted anomalous viscous-convective scaling is based on the assumption of a rather large nonhomogeneous contribution to  $\Psi$  that is suggestive of a strong vertical coherence. If this significant nonhomogeneous component exists, it should also be evident in the inertial-convective regime scaling. Efforts are currently under way to investigate nonhomogeneous, inertial-convective regime spatial correlations using the mean-field model. Future studies should lead to an improved understanding of the presence of intermittency and anisotropy in the statistics of a passive condensate which would be of particular relevance to the atmospheric science community.

## ACKNOWLEDGMENTS

I am grateful to Phillip Austin and Nicole Jeffery for a careful reading of the manuscript.

This work is supported by the Natural Sciences and Engineering Research Council of Canada and by the Izaak Walton Killam Memorial Predoctoral Fellowship.

<sup>1</sup>A. Davis, A. Marshak, H. Gerber, and W. J. Wiscombe, "Horizontal structure of marine boundary-layer clouds from centimeter to kilometer scales," *J. Geophys. Res.* **104**, 6123 (1999).

<sup>2</sup>A. Marshak, A. Davis, W. Wiscombe, and R. Cahalan, "Radiative effects

- of sub-mean free path liquid water variability observed in stratiform clouds," *J. Geophys. Res.* **103**, 19557 (1998).
- <sup>3</sup>R. A. Shaw, W. C. Reade, L. R. Collins, and J. Verlinde, "Preferential concentration of cloud droplets by turbulence: Effects on the early evolution of cumulus cloud droplet spectra," *J. Atmos. Sci.* **55**, 1965 (1998).
- <sup>4</sup>C. A. Jeffery, "Effect of particle inertia on the viscous-convective subrange," *Phys. Rev. E* **61**, 6578 (2000).
- <sup>5</sup>H. Gerber, J. B. Jensen, A. B. Davis, A. Marshak, and W. J. Wiscombe, "Spectral density of cloud LWC at high frequencies," *J. Atmos. Sci.* (to be published).
- <sup>6</sup>I. Mazin, "The effect of condensation and evaporation on turbulence in clouds," *Atmos. Res.* **51**, 171 (1999).
- <sup>7</sup>W. W. Grabowski, "Cumulus entrainment, fine-scale mixing, and buoyancy reversal," *Q. J. R. Meteorol. Soc.* **119**, 935 (1993).
- <sup>8</sup>G. L. Stephens and C. M. R. Platt, "Aircraft observations of the radiative and microphysical properties of stratocumulus and cumulus clouds fields," *J. Clim. Appl. Meteorol.* **26**, 1243 (1987).
- <sup>9</sup>V. R. Noonkester, "Droplet spectra observed in marine stratus cloud layers," *J. Atmos. Sci.* **41**, 829 (1984).
- <sup>10</sup>G. Vali, R. D. Kelly, J. French, S. Haimov, D. Leon, R. E. McIntosh, and A. Pazmany, "Finescale structure and microphysics of coastal stratus," *J. Atmos. Sci.* **55**, 3540 (1998).
- <sup>11</sup>Y. L. Kogan, M. P. Khairoutdinov, D. K. Lilly, Z. N. Kogan, and Q. Liu, "Modeling of stratocumulus cloud layers in a large eddy simulation model with explicit microphysics," *J. Atmos. Sci.* **52**, 2923 (1995).
- <sup>12</sup>B. Stevens, G. Feingold, W. R. Cotton, and R. L. Walko, "Elements of the microphysical structure of numerically simulated nonprecipitating stratocumulus," *J. Atmos. Sci.* **53**, 980 (1996).
- <sup>13</sup>M. F. Khairoutdinov and Y. L. Kogan, "A large eddy simulation model with explicit microphysics: Validation against aircraft observations of a stratocumulus-topped boundary layer," *J. Atmos. Sci.* **56**, 2115 (1999).
- <sup>14</sup>H. W. Barker, "Solar radiative transfer through clouds possessing isotropic variable extinction coefficient," *Q. J. R. Meteorol. Soc.* **118**, 1145 (1992).
- <sup>15</sup>W. I. Newman, J. K. Lew, G. L. Siscoe, and R. G. Fovell, "Systematic effects of randomness in radiative transfer," *J. Atmos. Sci.* **52**, 427 (1995).
- <sup>16</sup>M. Holzer and E. D. Siggia, "Turbulent mixing of a passive scalar," *Phys. Fluids* **6**, 1820 (1994).
- <sup>17</sup>A. Pumir, "A numerical study of the mixing of a passive scalar in three dimensions in the presence of a mean gradient," *Phys. Fluids* **6**, 2118 (1994).
- <sup>18</sup>C. Tong and Z. Warhaft, "On passive scalar derivative statistics in grid turbulence," *Phys. Fluids* **6**, 2165 (1994).
- <sup>19</sup>R. S. Miller, F. A. Jaber, C. K. Madnia, and P. Givi, "The structure and the small-scale intermittency of passive scalars in homogeneous turbulence," *J. Sci. Comput.* **10**, 151 (1995).
- <sup>20</sup>F. A. Jaber, R. S. Miller, C. K. Madnia, and P. Givi, "Non-gaussian scalar statistics in homogeneous turbulence," *J. Fluid Mech.* **313**, 241 (1996).
- <sup>21</sup>M. R. Overholt and S. B. Pope, "Direct numerical simulation of a passive scalar with imposed mean gradient in isotropic turbulence," *Phys. Fluids* **8**, 3128 (1996).
- <sup>22</sup>L. Mydlarski and Z. Warhaft, "Passive scalar statistics in high-Péclet-number grid turbulence," *J. Fluid Mech.* **358**, 135 (1998).
- <sup>23</sup>P. Hignett and J. P. Taylor, "The radiative properties of inhomogeneous boundary layer cloud: Observations and modeling," *Q. J. R. Meteorol. Soc.* **122**, 1341 (1996).
- <sup>24</sup>H. R. Pruppacher and J. D. Klett, *Microphysics of Clouds and Precipitation*, 2nd ed. (Kluwer Academic, Boston, 1997).
- <sup>25</sup>S. Nicholls and J. Leighton, "An observational study of the structure of stratiform cloud sheets: Part I. Structure," *Q. J. R. Meteorol. Soc.* **112**, 431 (1986).
- <sup>26</sup>P. Austin, Y. Wang, R. Pincus, and V. Kujala, "Precipitation in stratocumulus clouds: Observational and modeling results," *J. Atmos. Sci.* **52**, 2329 (1995).
- <sup>27</sup>P. G. Duynkerke, H. Zhang, and P. J. Jonker, "Microphysical and turbulent structure of nocturnal stratocumulus as observed during ASTEX," *J. Atmos. Sci.* **52**, 2763 (1995).
- <sup>28</sup>C.-H. Moeng, "Large-eddy simulation of a stratus-topped boundary layer. Part I: Structure and budgets," *J. Atmos. Sci.* **43**, 2886 (1986).
- <sup>29</sup>S. Wang and Q. Wang, "On condensation and evaporation in turbulence cloud parameterizations," *J. Atmos. Sci.* **56**, 3338 (1999).
- <sup>30</sup>D. Bogucki, J. Andrzej Domaradzki, and P. K. Yeung, "Direct numerical simulations of passive scalars with  $Pr > 1$  advected by turbulent flow," *J. Fluid Mech.* **343**, 111 (1997).
- <sup>31</sup>J. R. Chasnov, "The viscous-convective subrange in nonstationary turbulence," *Phys. Fluids* **10**, 1191 (1998).
- <sup>32</sup>R. H. Kraichnan, "Small-scale structure of a scalar field convected by turbulence," *Phys. Fluids* **11**, 945 (1968).
- <sup>33</sup>L. Piterbarg, "Short-correlation approximation in models of turbulent diffusion," in *Stochastic Models in Geosystems*, Vol. 85 of *IMA Volumes in Mathematics and its Applications*, edited by S. A. Molchanov and W. A. Woyczynski (Springer-Verlag, New York, 1997), pp. 313–352.
- <sup>34</sup>M. Avellaneda and A. J. Majda, "Simple examples with features of renormalization for turbulent transport," *Philos. Trans. R. Soc. London, Ser. A* **346**, 205 (1994).
- <sup>35</sup>Ya. B. Zeldovich, S. A. Molchanov, A. A. Ruzmaikin, and D. D. Sokoloff, "Intermittency, diffusion and generation in a nonstationary random medium," *Sov. Sci. Rev. C. Math. Phys.* **7**, 1 (1988).
- <sup>36</sup>J. O. Hinze, *Turbulence*, 2nd ed. (McGraw-Hill, New York, 1975).
- <sup>37</sup>G. K. Batchelor, "Small-scale variation of convected quantities like temperature in turbulent fluid. Part 1. General discussion and the case of small conductivity," *J. Fluid Mech.* **5**, 113 (1959).
- <sup>38</sup>R. C. Mjolsness, "Diffusion of a passive scalar at large Prandtl number according to the abridged Lagrangian interaction theory," *Phys. Fluids* **18**, 1393 (1975).
- <sup>39</sup>*Handbook of Mathematical Functions*, edited by M. Abramowitz and I. A. Stegun (Dover, New York, 1970).
- <sup>40</sup>S. Herr, L.-P. Wang, and L. R. Collins, "EDQNM model of a passive scalar with a uniform mean gradient," *Phys. Fluids* **8**, 1588 (1996).
- <sup>41</sup>J. R. Herring, "Approach of axisymmetric turbulence to isotropy," *Phys. Fluids* **17**, 859 (1974).
- <sup>42</sup>O. M. Phillips, "On the Bolgiano and Lumley-Shur theories of the buoyancy subrange," in *Atmospheric Turbulence and Radio Wave Propagation*, edited by A. M. Yaglom and V. I. Tatarsky (Nauka, Moscow, 1965), pp. 121–128.
- <sup>43</sup>J. L. Lumley, "The spectrum of nearly inertial turbulence in a stably stratified fluid," *J. Atmos. Sci.* **21**, 99 (1964).
- <sup>44</sup>J. Weinstock, "On the theory of temperature spectra in a stably stratified fluid," *J. Phys. Oceanogr.* **15**, 475 (1985).